

Measurement of the Energy Spectrum of a 6 MV Linear Accelerator Using Compton Scattering Spectroscopy and Monte Carlo-Generated Corrections

Sameer Taneja*, Laura J. Bartol, Wesley Culberson, Larry A. De Werd

School of Medicine and Public Health, University of Wisconsin-Madison, Madison, USA

Email: *sameer.taneja@nyulangone.org

How to cite this paper: Taneja, S., Bartol, L.J., Culberson, W. and De Werd, L.A. (2020) Measurement of the Energy Spectrum of a 6 MV Linear Accelerator Using Compton Scattering Spectroscopy and Monte Carlo-Generated Corrections. *International Journal of Medical Physics, Clinical Engineering and Radiation Oncology*, 9, 186-200. <https://doi.org/10.4236/ijmpcero.2020.94017>

Received: August 24, 2020

Accepted: October 17, 2020

Published: October 20, 2020

Copyright © 2020 by author(s) and Scientific Research Publishing Inc. This work is licensed under the Creative Commons Attribution International License (CC BY 4.0).

<http://creativecommons.org/licenses/by/4.0/>



Open Access

Abstract

Purpose: The energy spectrum of a linear accelerator used for dose calculations is determined during beam commissioning by iteratively adjusting the spectrum and comparing calculated and measured percent depth-dose curves. Direct measurement of the energy spectrum using pulse mode detectors is particularly challenging because of the high-energy, high fluence nature of these beams and limitations of the detector systems. This work implements a Compton scattering (CS) spectroscopy setup and presents detector corrections and spectral unfolding techniques to measure the spectrum of a 6 MV linear accelerator using a pulse mode detector. **Methods:** Spectral measurements were performed using a Varian Clinac 21EX linear accelerator and a high-purity germanium (HPGe) detector. To reduce fluence to the detector, a custom-built lead shield and a CS spectrometry setup were used. The detector was placed at CS angles of 46°, 89°, and 125°. At each of these locations, a detector response function was generated to account for photon interactions within the experimental geometry. Gold's deconvolution algorithm was used to unfold the energy spectrum. The measured spectra were compared to simulated spectra, which were obtained using an experimentally benchmarked model of the Clinac 21EX in MCNP6. **Results:** Measurements were acquired and detector response corrections were calculated for all three CS angles. A comparison of spectra for all CS angles showed good agreement with one another. The spectra for all three angles were averaged and showed good agreement with the MCNP6 simulated spectrum, with all points above 400 keV falling within 4%, which was within the uncertainty of the measurement and statistical uncertainty. **Conclusions:** The measurement of the energy spectrum of a 6 MV linear accelerator using a pulse-mode detector is pre-

sented in this work. For accurate spectrum determination, great care must be taken to optimize the detector setup, determine proper corrections, and to unfold the spectrum.

Keywords

Linear Accelerator, Energy Spectrum, Spectrometry, High Purity Germanium Detectors, Monte Carlo

1. Introduction

Dose calculation engines used in clinical radiation therapy treatment planning for photons primarily use model based dose calculation algorithms to determine dose to the patient [1] [2]. For these algorithms, the knowledge of the energy spectrum is important for accurate dose determination, especially around high-Z material interfaces and heterogeneities [3] [4] [5] [6] [7]. The spectrum is typically estimated by an iterative tuning approach [8] using beam data measured during linear accelerator commissioning [9]. An initial spectrum, determined through Monte-Carlo (MC) simulations or published beam data [10] [11], is iteratively adjusted until the calculated percent depth dose (PDD) curves match the measured PDDs in a standardized measurement setup [12].

The most common and widely accepted method for spectral determination of linear accelerators is through MC simulations. Linear accelerator models have been generated using various MC codes [1] [13]-[20]. It is known that there are differences among these codes including electron transport, bremsstrahlung cross sections, and variance reduction techniques [15] [16] [21], and as such it is recommended that these models are validated against measured beam data [22].

Measurement of the energy spectrum is challenging due to the high photon energy and high fluence rates that are characteristic of the output of the machines [23], and the limitations of detectors. As a result, spectrum measurements often implement techniques to reduce fluence to the detector and generate an environment in which measurements are feasible. A group of studies have inserted a target with a low-Z material, usually deuterium, into the primary photon beam, and measured the production of photoneutrons. Using cross-sectional data, the photon spectrum was determined [24] [25]. Faddegon *et al.* [26] decreased the mA of a clinical linear accelerator by several orders of magnitude, and used a pulse mode detector to measure the output spectrum. The most common technique for spectrum measurement involved unfolding an energy spectrum from measurements of beam transmission through various mass thicknesses of attenuating material [8] [27]-[34]. A photon energy spectrum can be subsequently unfolded from the transmission measurements using a wide variety of unfolding techniques, including Laplace transform pairs [3] [27] [31], direct matrix inversion [33], and neural networks [32].

Measurement of linear accelerator spectra using pulse mode detectors are li-

mitted by the processing speed of a spectroscopic system for a singular pulse [35]. The high fluence nature of linear accelerators induce pulse pile-up, in which pulses are often distorted or superimposed on top of one another, leading to inaccurate spectra measurements [23] [36]. Spectroscopic measurements of linear accelerator spectra were completed on first generation linear accelerators with accelerated electron energies ranging from (2 to 25) MeV using a Compton scattering technique [36]-[41]. Compton-scattering spectroscopy is performed by placing the pulse mode detector at a known angle from the primary axis, measuring a scatter spectrum, and calculating the primary spectrum [42] [43] [44] [45]. The authors corrected the response of the detectors using a response function and related the measured scatter spectra to the primary bremsstrahlung spectra using the Klein-Nishina cross section and the energy-angle relationship based on the assumption that electrons are unbound and at rest [23]. Response functions were typically generated through the interpolation of the response of monoenergetic sources or through analytical calculation. Both of these methods are limited by the availability and maximum energy of monoenergetic sources and the complexity of the collimation and shielding geometries used in calculations [23]. As a result, the agreement between measured and analytically determined spectra for first generation linear accelerators varied based on the effectiveness of the correction and unfolding techniques.

This work developed a technique to measure the spectrum of a 6 MV modern linear accelerator using a pulse mode detector in a CS geometry and a collimator. Monte Carlo simulations were used to determine a detector response function and to determine the primary spectrum from the scatter spectrum taking into account bound electrons. The measured spectrum was compared with Monte Carlo simulations using a linear accelerator model that was validated against beam data.

The upcoming sections will describe the complete measurement and simulation setup, which include the generation and application of the detector response function and the implementation of unfolding techniques. Finally, a comparison between measurements and simulations is presented to show the accuracy of the measurement technique.

2. Materials and Methods

2.1. Measurement Setup

Measurements were performed using a 6 MV Varian Clinac[®] 21EX (Varian Medical Systems, Palo Alto CA) at the University of Wisconsin Medical Radiation Research Center (UWMRRC). A reverse electrode, high-purity germanium (HPGe) pulse mode detector (Canberra Industries, Meriden CT) cooled to 77 K using liquid nitrogen was used for measurement. Radiation interactions in HPGe detectors generate electron-hole pairs in an amount that is proportional to the incident particle's energy [35]. The measured signal from the HPGe was processed using Nuclear Instrumentation Module (NIM) components including a pream-

plifier and amplifier for signal shaping, an analog-to-digital converter to assign a numerical value per signal shape, and a multi-channel analyzer for binning pulses based on their digital value (Canberra Industries, Meriden CT). The raw measurement, post signal processing, was in the form a pulse-height distribution (PHD), and was recorded using the Genie T2000™ software (Canberra Industries, Meriden CT). An energy calibration was performed for the HPGe using a ^{152}Eu standard source [46] [47].

The HPGe detector was placed in a custom-built, cylindrical lead shield that provided 10 cm of lead around the detector, and 30 cm of lead in front of the detector. The inside cavity was lined with a 0.08 cm layer of tin and a 0.15 cm layer of copper to eliminate the contribution of fluorescent photon signal that is produced from interactions in the shield. A tungsten collimating insert was placed into the shield and provided a 2 mm in-diameter aperture [23].

A photograph of the measurement setup is shown in **Figure 1**. The detector and shield were positioned at three Compton-scattering angles including 46° , 89° , and 125° from the beam's central axis. The shield's aperture was aligned to machine isocenter using a series of matched lasers that attached to the front face and the back cavity of the lead shield. A cylindrical scattering rod made of high-grade aluminum with dimensions of 2.5 cm in-diameter and 5 cm in height was placed at isocenter.

PHD measurements were performed with the linear accelerator set to an energy of 6 MV, a dose rate of 600 MU/min, a beam on time of 60 minutes, a field size of (5×5) cm² to limit photons not interacting with the scattering rod, and with the MLCs retracted. In order to account for scattered photons that penetrated the detector shield, a background measurement was performed with

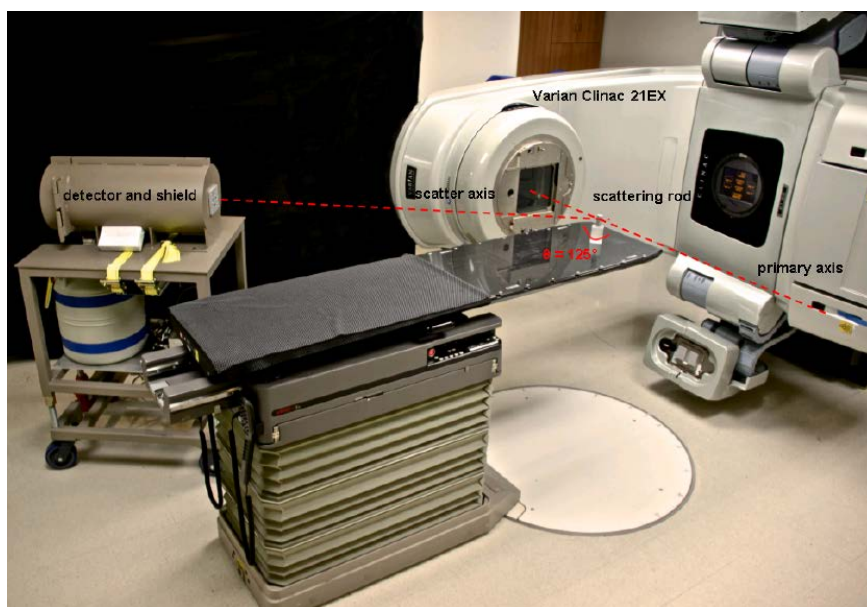


Figure 1. Photographs of the Compton-scattering spectrometry setup used for spectra measurements of the Varian Clinac 21EX linear accelerator. The image shows the setup for a CS angle of 125° .

identical settings on the linear accelerator, but with the pinhole collimator plugged with a 6-inch tungsten rod. The background measurement was subtracted from the PHD in order to isolate the intended signal.

2.2. Spectrum Processing

A detector response function (DRF) was implemented to account for the geometry of the HPGe detector and the location of the detector and shield with respect to the primary radiation beam. The DRF was generated using Monte Carlo N-particle transport (MCNP) Version 6 [48]. A model of the HPGe detector and shield was adapted from previous work by Bartol [23], which validated the geometry for high energy photons. A cross sectional view of the detector and shield geometry, including the collimator, crystal, window, tin and copper detector housing, and (p.n) contacts, is shown in **Figure 2** using Visual Editor (VisEd) (Schwarz Software and Consulting LCC, Richland WA).

Monoenergetic photons were simulated through the experimental geometry, shown in **Figure 3**, and the individual detector responses resulting from each photon energy were combined to form a DRF matrix that were subsequently used for correction. For each individual simulation, a series of variance reduction techniques were implemented to selectively track particles that scatter toward the germanium detector. In addition, Doppler broadening was measured using a standard source and implemented in simulations to account for statistical peak broadening in spectroscopy [44]. **Figure 4** shows a three-dimensional plot of the DRF matrix for a CS angle of 125° , where the x-axis represents the starting energy for all photons in the simulations, the y-axis shows the measured photon energy, and the z-axis shows the total number of pulses normalized to a starting particle. The majority of the contribution to the scatter spectrum at 125° angle originate from lower energy photons along the primary axis as higher energy photons scatter in a more forward direction [49]. Each CS angle measurement

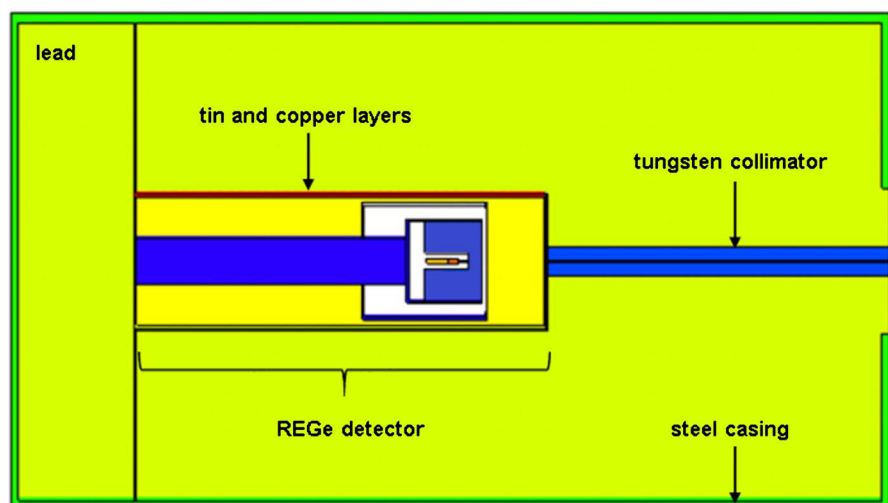


Figure 2. A VisEd rendering of the UWMRRC HPGe detector inside a custom built lead shielding with a tungsten collimator.

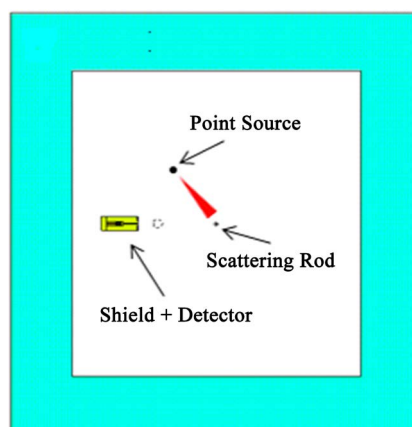


Figure 3. A VisEd rendering of the simulation geometry used to generate a detector response function.

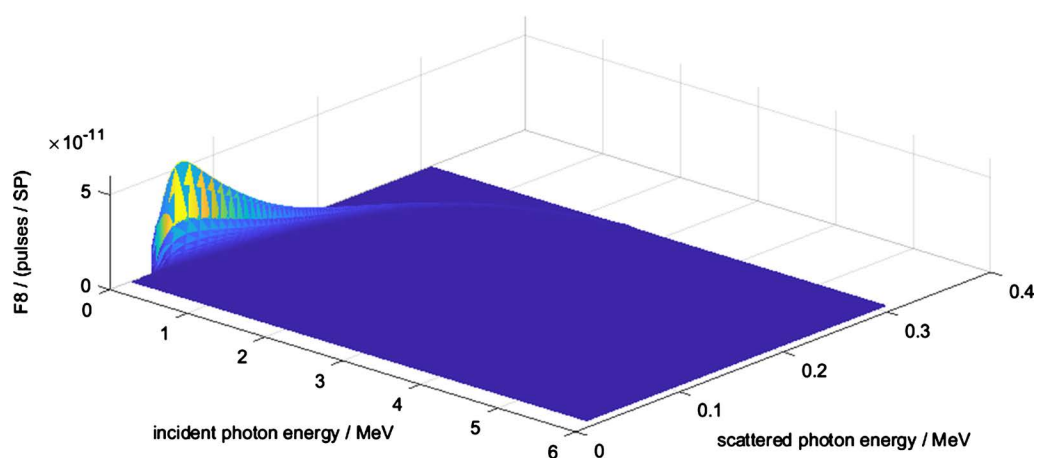


Figure 4. Three-dimensional plot of the detector response function for a Compton-scattering angle of 125° .

required a unique DRF that was descriptive of those individual setup parameter (*i.e.* detector distance to isocenter, vault walls, etc.).

The detector response function was applied to the measured scatter spectrum using an iterative spectral unfolding method that follows Gold's deconvolution, which was described by Bandzuch *et al.* [50] and applied to spectral deconvolution by Beach and DeWerd. [51] This method is a favorable deconvolution technique by minimizing non-negative solutions [52] [53].

2.3. Monte-Carlo Methods

A model of the Clinac 21EX linear accelerator with a (5×5) cm² field size was generated in MCNP6 and used to simulate spectra that were used for comparison with measurements. The physical components of the linear accelerator were modeled using the manufacturer's schematics (Varian Medical Systems). The MLCs were not modeled, as all measurements were performed using jaw-defined fields. The model was benchmarked using methods described from the recommendations from beam parameter sensitivity studies [17] [54] [55]. An optimal

electron energy and spot size were determined in a piecemeal fashion through the comparison of simulated and measured percent depth dose (PDD) curves and field profiles. Electron energies of (5.7, 5.8, 5.9, 6.0, 6.1, and 6.2) MeV and spot sizes of (0.06, 0.08, 0.10, 0.12, 0.14, and 0.16) cm were investigated. Beam data was measured using an Exradin A12 farmer-type ionization chamber (Standard Imaging, Middleton WI) in a Doseview 3D water tank (Standard Imaging). The optimal electron energy and spot sizes were determined using a root-mean-square deviation test. The spectrum was scored using a fluence tally (F5) located at a point along the beam's central axis and below the jaws where the measured and simulated spectra were compared.

2.4. Post Processing

Post application of response corrections and spectral unfolding, the resulting spectra were smoothed using a moving average filter. The energy resolution of the deconvolved energy spectrum was dependent on the CS angle. This is because the energy resolution of the PHD remained the same, so the total number of energy bins ranged from about 500 to 2500 based on CS angle. As the angle increased from 46° to 125°, the measured PHD's maximum energy decreased from 395 keV to 1300 keV. The total number of monoenergetic simulations used to generate a PHD as well as the total number of energy bins in the final deconvolved spectrum ranged from 500 to 2500. For comparison of measured spectra with one another, a cubic spline interpolation was performed to obtain the energy resolution of 100 keV. **Figure 5** shows the smoothed and interpolated measured spectra for all three CS angles, normalized to maximum peak energy.

3. Results and Discussion

Figure 5 presents the three CS spectra were corrected using unique detector response functions and unfolded separately. Detector pileup was minimal given the measurement setup, as there was no counts above background greater than the maximum expected energy. In addition, the deadtime for the PHD measurements ranged from 0.5% to 4%, indicating that the collimation and CS technique limited counts to the detector. The maximum deviation between the measured spectra was 8% above the low energy, high gradient region (above 400 keV).

The overall uncertainty and the individual contributors to that uncertainty are presented in **Table 1** for a sample point along the spectrum at 1.20 MeV. The greatest source of uncertainty was the Type A statistical uncertainty for the PHD measurement, which was determined by counting statistics and had a magnitude of 5.2%. The energy calibration Type B uncertainty was determined by the accuracy of the energy calibration fit, and the Type A uncertainty was provided by the counting statistics for the calibration measurement. Linear accelerator output over the course of 60 minutes is stable, and the PHD measurements used for comparison were identical in time. The Type A uncertainty in the simulation of

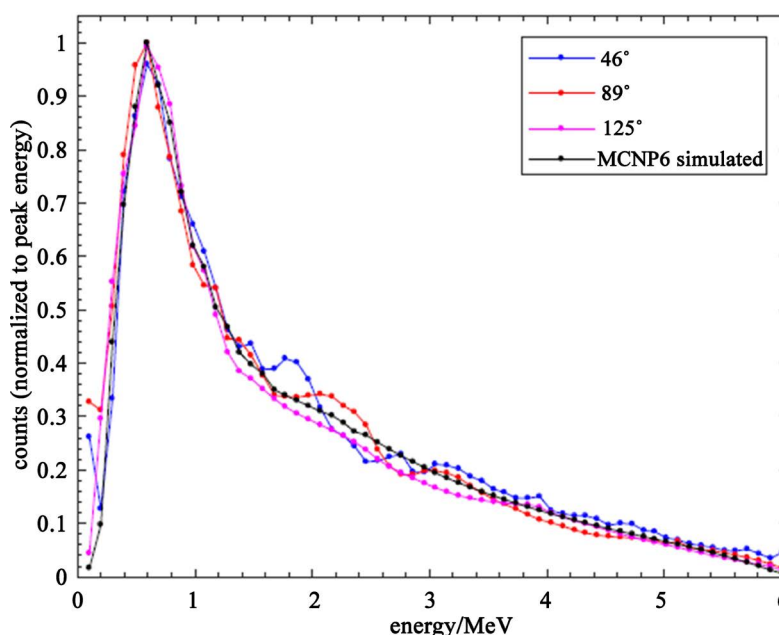


Figure 5. Measured energy spectrum of a 6 MV Clinac 21EX for three Compton-scattering angles (colors) and simulated energy spectrum (black).

Table 1. Sample uncertainty analysis for energy bin at 1.20 MeV.

Parameter	Type A	Type B
Detector energy calibration (^{152}Eu)	0.1%	0.3%
Pulse-height distribution measurement	5.2%	
Linear accelerator output	0.0%	
Detector positioning*		90.0%/1°
Detector response function simulations	0.7%	0.5%
Gold's deconvolution		1.1%
A and B Quad sum	5.25%	1.24%
Total combined uncertainty	(k = 1)	5.39%
Expanded total uncertainty	(k = 2)	10.78%

*The detector position was iteratively adjusted for maximum signal during measurement. Based on the total signal output the relative uncertainty was about 10%/1°.

the DRF was set as the MCNP generated statistical uncertainty and the Type B uncertainty was determined by varying the material composition of the scattering rod, which changes the scattering properties. The detector positioning uncertainty was determined as 90% per 1° (90%/1°), which was determined by slightly moving the position of the detector and determining the decrease in overall intended signal. This was not accounted for in the overall uncertainty as the detector was positioned to maximize signal to the detector, which occurs when there is a line of sight to the scattering rod through the collimator. The reproducibility of the detector setup was demonstrated by the three setup angles that were used. The overall uncertainty at the energy bin at 1.20 MeV is 10.8% at

the $k = 2$ (95% confidence interval) level.

A model of the Varian Clinac 21EX in MCNP6 was validated against PDD and cross-field profile measurements by determining the optimal incident electron energy and spot size. **Figure 6(a)** plots the measured PDD along with the simulated PDDs corresponding to all incident electron energies investigated in this work along. **Figure 6(c)** plots the measured cross-field profile as well as simulated cross-field profiles corresponding to the electron spot sizes and the measured profile. Profile residuals are shown in **Figure 6(b)** and **Figure 6(d)**. After performing a RMSD test, it was found that the optimal electron energy was 6.0 MeV and the optimal spot size was 0.12 cm. These values were representative of previous studies [17], and were used for all spectrum simulations in this work.

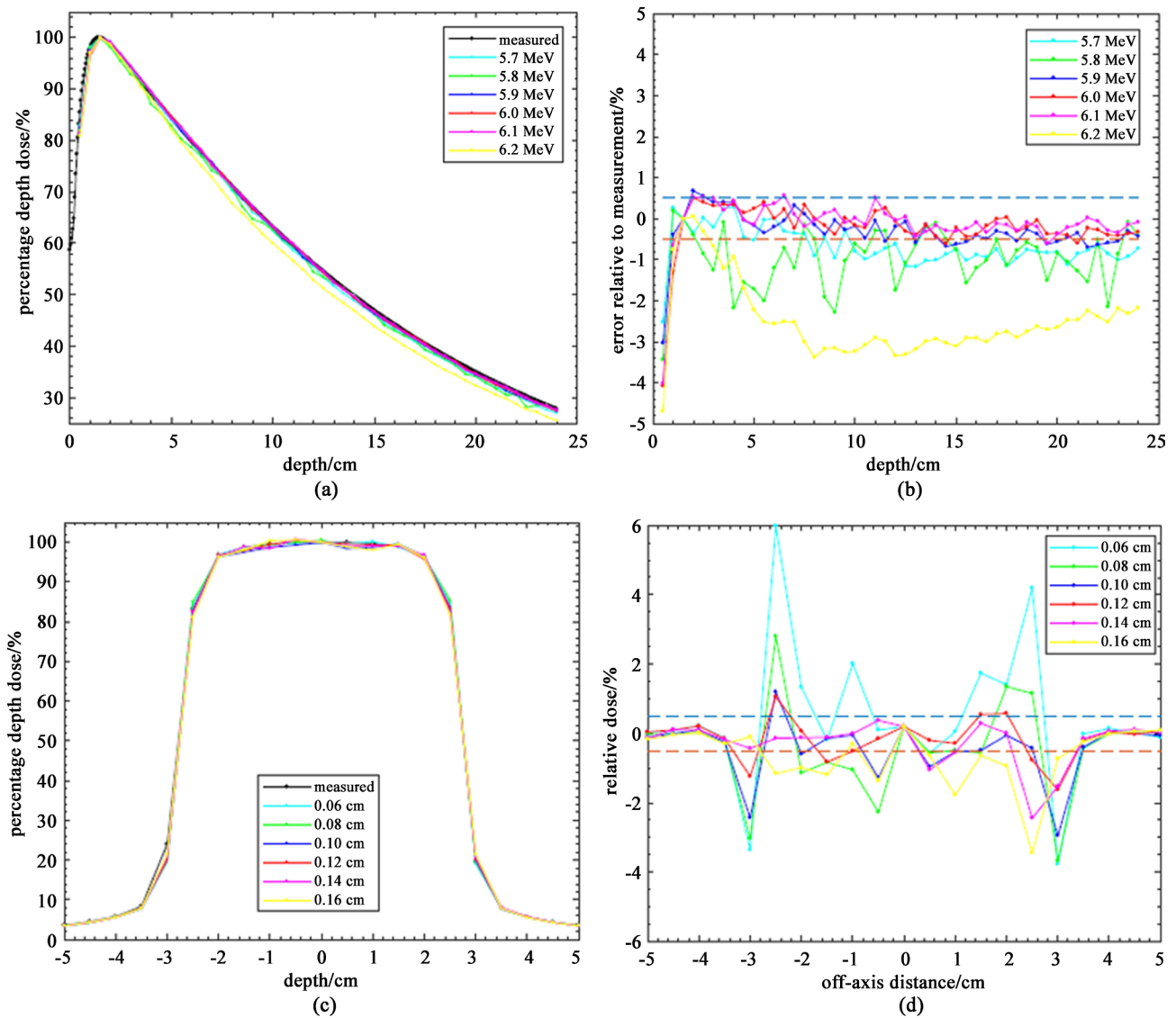


Figure 6. Determination of optimal beam parameters for the MCNP6 model of the Varian Clinac 21EX. (a) PDDs corresponding to electron energies ranging from 5.7 MeV to 6.2 MeV, and (b) Residuals calculated by subtracting the measured PDD from the simulated PDD. (c) Cross-field profiles and (d) Residuals, for electron spot sizes ranging from 0.06 cm to 0.16 cm. Measured PDDs and profiles are in black.

A bin-to-bin average of the three spectra was calculated and compared with the MC-generated spectrum, shown in **Figure 7(a)**. The simulated spectrum showed good agreement with the measured average spectrum. **Figure 7(b)** shows a bin-to-bin subtraction between the simulated and measured spectra to show residuals. Above the high-gradient region, >400 keV, the measured and simulated spectra agreed to within 4%, which was well within the propagated uncertainty between the measurements and simulations.

4. Discussion

This work demonstrated the feasibility to measure the energy spectrum of a 6 MV linear accelerator using a pulse mode detector in a CS spectroscopy setup and Monte Carlo corrections. Three independent measurements were taken at different CS angles and were uniquely corrected for the response and probability of scattered photon to determine the spectrum along the central axis. The agreement between the final spectra between the three CS angle measurements provided confidence in the methods that were implemented for DRF corrections and spectral unfolding. In addition, the agreement between the measured spectra and Monte Carlo simulations validated the accuracy of the measured spectrum.

The setup of the pulse mode detector was important in the measurement as shielding and collimation were necessary to avoid detector pulse pileup. The low deadtime and the lack of presence of added pulses indicated that the shielding was adequate. The high statistical uncertainty due to counting statistics indicated that the detector was over-shielded, and less extensive shielding would suffice. The relatively low count rate with regard to the maximum detectable count rate of a pulse mode detector indicates that the presented measurement setup could be used for spectral measurements for higher fluence sources including flattening

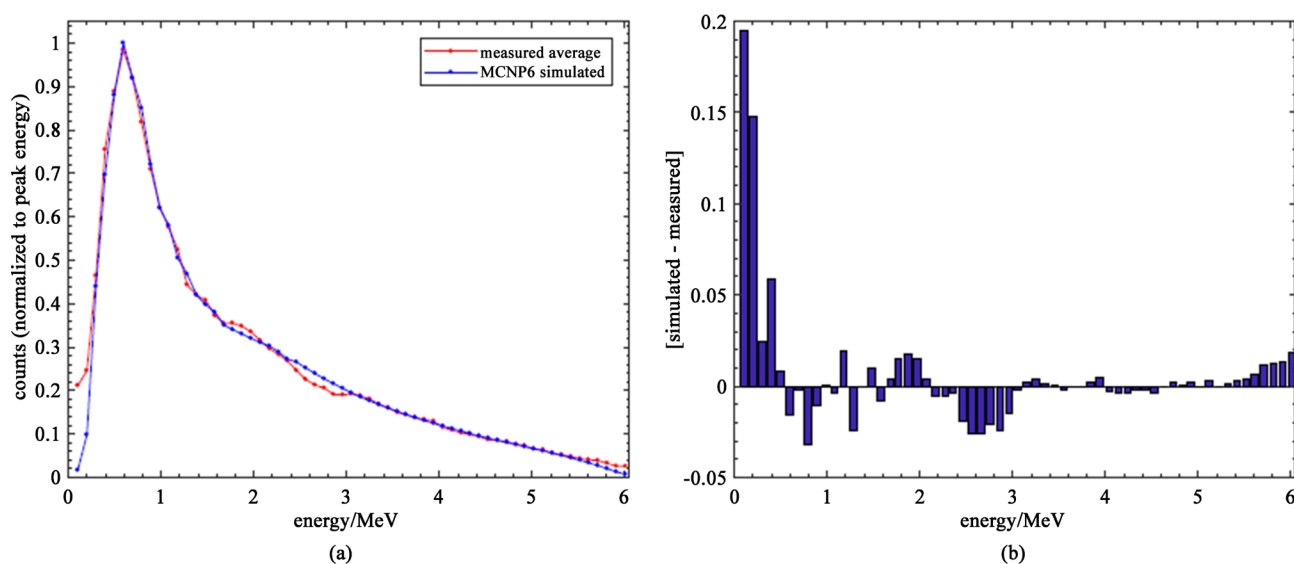


Figure 7. (a) Interpolated measured energy spectrum of a 6 MV linear accelerator averaged for all three Compton-scattering angles and compared with the MCNP6 simulations, and (b) Residuals from a bin-to-bin subtraction of the measured spectrum from the simulated spectrum.

filter free beams.

The spectral processing techniques were adapted from previous work developed by Beach and De Werd [51] for a CS spectroscopy setup and with detector shielding in a high energy, high fluence measurement. The complexity of the DRF simulations required thorough implementation of variance reduction (VR) and understanding of MCNP6 geometries. VR techniques reduced the time required for each simulation, and on average 200 monoenergetic simulations were completed per day on a high performance computing cluster that runs MCNP simulations via a parallel CPU-based architecture. The geometry of each part of the Monte-Carlo simulation was validated against measurements, including the detector and shield [23] and the directional scattering of photons off of the scattering rod using DXTRAN spheres [56] [57] [58]. The DRF was critical in correcting the PHD for the geometry of the experimental setup, and the agreement between the spectra at different CS angles provides confidence in the DRF generation method.

The agreement of the measured energy spectra with MC simulations provided validation in the measurements with the current gold standard for determining the energy spectrum of linear accelerators. The presented method requires significant equipment and time, but presents a method that measures a pulse-height distribution, which is a combination of singular photon counts and can be related to an energy spectrum. Other measurement techniques measure a secondary quantity (*i.e.* charge) and calculate the energy spectrum. The authors do not envision direct measurement as part of the commissioning process due to the practicality of the presented work, but encourage the use of the measurement techniques for validating simulations or indirect measurements. Optimization of the presented method could prove valuable in validating Monte Carlo simulations of output energy spectrum for new technologies.

Acknowledgements

The authors would like to thank John Micka and Cliff Hammer for their assistance with measurements as well as all students at the UWMRRC for their input and support of this work. The author's would also like to thank the University of Wisconsin Accredited Dosimetry Calibration Laboratory (UWADCL) and the University of Wisconsin Radiation Calibration Laboratory (UWRCL) customers, whose calibrations help support ongoing research at the UWMRRC.

Conflicts of Interest

The authors declare no conflicts of interest regarding the publication of this paper.

References

- [1] Mohan, R., Chui, C. and Lidofsky, L. (1985) Energy and Angular Distributions of Photons from Medical Linear Accelerators. *Medical Physics*, **12**, 592-597. <https://doi.org/10.1118/1.595680>

- [2] Papanikolaou, N., Mackie, T.R., Meger-Wells, C., Gehring, M. and Reckwerdt, P. (1993) Investigation of the Convolution Method for Polyenergetic Spectra. *Medical Physics*, **20**, 1327-1336. <https://doi.org/10.1118/1.597154>
- [3] Werner, B.L. (1991) Dose Perturbations at Interfaces in Photon Beams: Annihilation Radiation. *Medical Physics*, **18**, 713-718. <https://doi.org/10.1118/1.596664>
- [4] Das, I.J., Moskvina, V.P., Kassaei, A., Tabata, T. and Verhaegen, F. (2002) Dose Perturbations at High-Z Interfaces in Kilovoltage Photon Beams: Comparison with Monte Carlo Simulations and Measurements. *Radiation Physics and Chemistry*, **64**, 173-179. [https://doi.org/10.1016/S0969-806X\(01\)00460-1](https://doi.org/10.1016/S0969-806X(01)00460-1)
- [5] Charland, P.M., Chetty, I.J., Paniak, L.D., Bednarz, B.P. and Fraass, B.A. (2004) Enhanced Spectral Discrimination through the Exploitation of Interface Effects in Photon Dose Data. *Medical Physics*, **31**, 264-276. <https://doi.org/10.1118/1.1637731>
- [6] Chibani, O. and Li, X.A. (2002) Monte Carlo Dose Calculations in Homogeneous Media and at Interfaces: A Comparison between GEPTS, Egsnrc, MCNP, and Measurements. *Medical Physics*, **29**, 835-847. <https://doi.org/10.1118/1.1473134>
- [7] Das, I.J. and Kahn, F.M. (1989) Backscatter Dose Perturbation at High Atomic Number Interfaces in Megavoltage Photon Beams. *Medical Physics*, **16**, 367-375. <https://doi.org/10.1118/1.596345>
- [8] Ali, E.S.M. and Rogers, D.W.O. (2012) An Improved Physics-Based Approach for Unfolding Megavoltage Bremsstrahlung Spectra Using Transmission Analysis. *Medical Physics*, **39**, 1663-1675. <https://doi.org/10.1118/1.3687164>
- [9] Das, I.J., Cheng, C.W., Watts, R.J., et al. (2008) Accelerator Beam Data Commissioning Equipment and Procedures: Report of the TG-106 of the Therapy Physics Committee of the AAPM. *Medical Physics*, **35**, 4186-4125. <https://doi.org/10.1118/1.2969070>
- [10] Glide-Hurst, C., Bellon, M., Foster, R., et al. (2013) Commissioning of the Varian TrueBeam Linear Accelerator: A Multi-Institutional Study. *Medical Physics*, **40**, Article ID: 031719.
- [11] Beyera, G.P. (2013) Commissioning Measurements for Photon Beam Data on Three Truebeam Linear Accelerators, and Comparison with Trilogy and Clinac 2100 Linear Accelerators. *Journal of Applied Clinical Medical Physics*, **14**, 273-288. <https://doi.org/10.1120/jacmp.v14i1.4077>
- [12] Starkschall, G., Steadham, R.E., Popple, R.A., Ahmad, S. and Rosen, I.I. (2000) Beam-Commissioning Methodology for a Three-Dimensional Convolution/Superposition Photon Dose Algorithm. *Journal of Applied Clinical Medical Physics*, **1**, 8-27.
- [13] Lovelock, D.M.J., Chui, C.S. and Mohan, R. (1995) A Monte Carlo Model of Photon Beams Used in Radiation Therapy. *Medical Physics*, **22**, 1387-1394. <https://doi.org/10.1118/1.597620>
- [14] Rogers, D.W.O., Faddegon, B.A., Ding, G.X., Ma, C.M., We, J. and Mackie, T.R. (1995) BEAM: A Monte Carlo Code to Simulate Radiotherapy Treatment Units. *Medical Physics*, **22**, 503-524. <https://doi.org/10.1118/1.597552>
- [15] Libby, B., Siebers, J. and Mohan, R. (1999) Validation of Monte Carlo Generated Phase-Space Descriptions of Medical Linear Accelerators. *Medical Physics*, **26**, 1476-1483. <https://doi.org/10.1118/1.598643>
- [16] Siebers, J.V., Keall, P.J., Libby, B. and Mohan, R. (1999) Comparison of EGS4 and MCNP4b Monte Carlo Codes for Generation of Photon Phase Space Distributions for a Varian 2100C. *Physics in Medicine & Biology*, **44**, 3009-3026. <https://doi.org/10.1088/0031-9155/44/12/311>
- [17] Sheikh-Bagheri, D. and Rogers, D.W.O. (2002) Sensitivity of Megavoltage Photon

- Beam Monte Carlo Simulations to Electron Beam and Other Parameters. *Medical Physics*, **29**, 379-390. <https://doi.org/10.1118/1.1446109>
- [18] Kry, S.F., Titt, U., Pönisch, F., et al. (2006) a Monte Carlo Model for Calculating Out-of-Field Dose from a Varian 6 MV Beam. *Medical Physics*, **33**, 4405-4413. <https://doi.org/10.1118/1.2360013>
- [19] Demarco, J.J., Solberg, T.D. and Smathers, J.B. (1998) A CT-Based Monte Carlo Simulation Tool for Dosimetry Planning and Analysis. *Medical Physics*, **25**, 1-11. <https://doi.org/10.1118/1.598167>
- [20] Lewis, R.D., Ryde, S.J.S., Hancock, D.A. and Evans, C.J. (1999) An MCNP-Based Model of a Linear Accelerator X-Ray Beam. *Physics in Medicine & Biology*, **44**, 1219-1230. <https://doi.org/10.1088/0031-9155/44/5/010>
- [21] Faddegon, B.A., Asai, M., Perl, J., et al. (2008) Benchmarking of Monte Carlo Simulation of Bremsstrahlung from Thick Targets at Radiotherapy Energies. *Medical Physics*, **35**, 4308-4317. <https://doi.org/10.1118/1.2975150>
- [22] Verhaegen, F. and Seuntjens, J. (2003) Monte Carlo Modelling of External Radiotherapy Photon Beams. *Physics in Medicine & Biology*, **48**, R107-64. <https://doi.org/10.1088/0031-9155/48/21/R01>
- [23] Bartol, L.J. (2013) Spectroscopic Characterization of High-Energy and High-Fluence Rate Photon Beams. The University of Wisconsin, Madison.
- [24] O'Dell, A.A., Sandifer, C.W., Knowlen, R.B. and George, W.D. (1968) Measurement of Absolute Thick-Target Bremsstrahlung Spectra. *Nuclear Instruments and Methods*, **61**, 340-346. [https://doi.org/10.1016/0029-554X\(68\)90248-6](https://doi.org/10.1016/0029-554X(68)90248-6)
- [25] Lambert, R.P., Jury, J.W. and Sherman, N.K. (1983) Measurement of Bremsstrahlung Spectra from 25 MeV Electrons on Ta as a Function of Radiator Thickness and Emission Angle. *Nuclear Instruments and Methods in Physics Research*, **214**, 349-360. [https://doi.org/10.1016/0167-5087\(83\)90602-6](https://doi.org/10.1016/0167-5087(83)90602-6)
- [26] Faddegon, B.A. (1990) Pile-Up Corrections in Pulsed-Beam Spectroscopy. *Nuclear Instruments and Methods in Physics Research Section B: Beam Interactions with Materials and Atoms*, **51**, 431-441. [https://doi.org/10.1016/0168-583X\(90\)90564-B](https://doi.org/10.1016/0168-583X(90)90564-B)
- [27] Huang, P., Kase, K.R. and Bjärngard, B.E. (1981) Spectral Characterization of 4 MV Bremsstrahlung by Attenuation Analysis. *Medical Physics*, **8**, 368-374. <https://doi.org/10.1118/1.594959>
- [28] Baker, C.R., Ama'ee, B. and Spyrou, N.M. (1995) Reconstruction of Megavoltage Photon Spectra by Attenuation Analysis. *Physics in Medicine & Biology*, **40**, 529-542. <https://doi.org/10.1088/0031-9155/40/4/004>
- [29] Ahuja, S.D., Steward, P.G., Roy, T.S. and Slessinger, E.D. (1986) Estimated Spectrum of a 4-MV Therapeutic Beam. *Medical Physics*, **13**, 368-373. <https://doi.org/10.1118/1.595878>
- [30] Archer, B.R., Almond, P.R. and Wagner, L.K. (1985) Application of Laplace Transform Pair Model for High-Energy X-Ray Spectral Reconstruction. *Medical Physics*, **12**, 630-633. <https://doi.org/10.1118/1.595684>
- [31] Scouarnec, C. and Catala, A. (1993) Simulation of X-Ray Spectral Reconstruction from Transmission Data by Direct Resolution of the Numeric System $AF=T$. *Medical Physics*, **20**, 1695-1703.
- [32] Hussain, S. (2010) Artificial Neural Network Model for Spectral Construction of a Linear Accelerator Megavoltage Photon Beam. 2010 *International Conference on Intelligent Systems, Modelling and Simulation*, Liverpool, 27-29 January 2010, 86-91. <https://doi.org/10.1109/ISMS.2010.27>

- [33] Waggener, R.G., Blough, M.M., Terry, J.A., et al. (1999) X-Ray Spectra Estimation Using Attenuation Measurements from 25 kVp to 18 MV. *Medical Physics*, **26**, 1269-1278. <https://doi.org/10.1118/1.598622>
- [34] Choi, H.J., Park, H., Yi, C.Y., Kim, B.C., Shin, W.G. and Min, C.H. (2019) Determining the Energy Spectrum of Clinical Linear Accelerator Using an Optimized Photon Beam Transmission Protocol. *Medical Physics*, **46**, 3285-3297. <https://doi.org/10.1002/mp.13569>
- [35] Knoll, G.F. (2000) Radiation Detection and Measurement. Wiley.
- [36] Levy, L.B., Waggener, R.G. and Wright, A.E. (1976) Measurement of Primary Bremsstrahlung Spectrum from an 8 MeV Linear Accelerator. *Medical Physics*, **3**, 173-175. <https://doi.org/10.1118/1.594221>
- [37] Levy, L.B., Waggener, R.G., McDavid, W.D. and Payne, W.H. (1974) Experimental and Calculated Bremsstrahlung Spectra from a 25 MeV Linear Accelerator and a 19 MeV Betatron. *Medical Physics*, **1**, 62-67. <https://doi.org/10.1118/1.1637280>
- [38] Anderson, D.W. (1991) Measurement of Accelerator Bremsstrahlung Spectra with a High-Efficiency Ge Detector. *Medical Physics*, **18**, 527-532. <https://doi.org/10.1118/1.596658>
- [39] Jessen, K.A. (1973) Measurements of Primary Spectra from a Kilocurie ⁶⁰Co Unit and a 6 MeV Linear Accelerator. *Acta Radiologica: Therapy, Physics, Biology*, **12**, 561-568. <https://doi.org/10.3109/02841867309130421>
- [40] Brownridge, J., Samnick, S., Stiles, P., Tipton, P., Veselka, J. and Yeh, N. (1984) Determination of the Photon Spectrum of a Clinical Accelerator. *Medical Physics*, **11**, 794-796. <https://doi.org/10.1118/1.595582>
- [41] Bentley, R.E., Jones, J.C. and Lillicrap, S.C. (1967) X-Ray Spectra from Accelerators in the Range 2 to 6 MeV. *Physics in Medicine & Biology*, **12**, 301-314. <https://doi.org/10.1088/0031-9155/12/3/302>
- [42] Yaffe, M., Taylor, K.W. and Johns, H.E. (1976) Spectroscopy of Diagnostic X Rays by a Compton Scatter Method. *Medical Physics*, **3**, 328-334. <https://doi.org/10.1118/1.594263>
- [43] Matscheko, G. and Carlsson, G.A. (1989) Measurement of Absolute Energy Spectra from a Clinical CT Machine under Working Conditions Using a Compton Spectrometer. *Physics in Medicine & Biology*, **34**, 209-222. <https://doi.org/10.1088/0031-9155/34/2/005>
- [44] Matscheko, G. and Carlsson, G.A. (1989) Compton Spectroscopy in the Diagnostic X-Ray Energy Range: I. Spectrometer Design. *Physics in Medicine & Biology*, **34**, 185-197. <https://doi.org/10.1088/0031-9155/34/2/003>
- [45] Matscheko, G., Carlsson, G.A., and Ribberfors, R. (1989) Compton Spectroscopy in the Diagnostic X-Ray Energy Range: II. Effects of Scattering Material and Energy Resolution. *Physics in Medicine & Biology*, **34**, 199-208. <https://doi.org/10.1088/0031-9155/34/2/004>
- [46] Castro, R.M., Vanin, V.R., Pascholati, P.R., Maidana, N.L., Dias, M.S. and Koskinas, M.F. (2004) Developing ¹⁵²Eu into a Standard for Detector Efficiency Calibration. *Applied Radiation and Isotopes*, **60**, 283-287. <https://doi.org/10.1016/j.apradiso.2003.11.029>
- [47] Taneja, S., Bartol, L.J., Culberson, W.S. and Dewerd, L.A. (2018) Characterization of the Energy Spectrum of a ¹³⁷Cs Irradiator through Measurements Using a Pulse-Mode Detector. *Radiation Measurements*, **114**, 1-7. <https://doi.org/10.1016/j.radmeas.2018.04.004>

- [48] Goorley, T., James, M., Booth, T., et al. (2012) Initial MCNP6 Release Overview. *Nuclear Technology*, **180**, 298-315.
- [49] Attix, F.H. (1986) Introduction to Radiological and Radiation Dosimetry. Wiley-VCH, Weinheim.
- [50] Bandžuch, P., Morháč, M. and Krištiak, J. (1997) Study of the Van Cittert and Gold Iterative Methods of Deconvolution and Their Application in the Deconvolution of Experimental Spectra of Positron Annihilation. *Nuclear Instruments and Methods in Physics Research Section A: Accelerators, Spectrometers, Detectors and Associated Equipment*, **384**, 506-515. [https://doi.org/10.1016/S0168-9002\(96\)00874-1](https://doi.org/10.1016/S0168-9002(96)00874-1)
- [51] Beach, S.M. and Dewerd, L.A. (2007) Deconvolution and Reconstruction Techniques of Closely Spaced Low-Energy Spectra from High-Purity Germanium Spectrometry. *Nuclear Instruments and Methods in Physics Research Section A: Accelerators, Spectrometers, Detectors and Associated Equipment*, **572**, 794-803. <https://doi.org/10.1016/j.nima.2006.12.006>
- [52] Morháč, M., Kliman, J., Matoušek, V., Veselský, M. and Turzo, I. (1997) Efficient One- and Two-Dimensional Gold Deconvolution and Its Application to γ -Ray Spectra Decomposition. *Nuclear Instruments and Methods in Physics Research Section A: Accelerators, Spectrometers, Detectors and Associated Equipment*, **401**, 385-408. [https://doi.org/10.1016/S0168-9002\(97\)01058-9](https://doi.org/10.1016/S0168-9002(97)01058-9)
- [53] Morháč, M., Matoušek, V. and Kliman, J. (2003) Efficient Algorithm of Multidimensional Deconvolution and Its Application to Nuclear Data Processing. *Digital Signal Processing*, **13**, 144-171. [https://doi.org/10.1016/S1051-2004\(02\)00011-8](https://doi.org/10.1016/S1051-2004(02)00011-8)
- [54] Chibani, O., Moftah, B. and Ma, C. (2010) SU-GG-T-402: On Monte Carlo Modeling of Megavoltage Photon Beams: A Revisited Study on Beam Parameters Sensitivity. *Medical Physics*, **37**, 3278-3279. <https://doi.org/10.1118/1.3468799>
- [55] Almberg, S.S., Frengen, J. and Lindmo, T. (2012) Monte Carlo Study of In-Field and Out-of-Field Dose Distributions from a Linear Accelerator Operating with and without a Flattening-Filter. *Medical Physics*, **39**, 5194-5203. <https://doi.org/10.1118/1.4738963>
- [56] Booth, T.E., Kelley, K.C. and Mccready, S.S. (2009) Monte Carlo Variance Reduction Using Nested Dextran Spheres. *Nuclear Technology*, **168**, 765-767. <https://doi.org/10.13182/NT09-A9303>
- [57] Booth, T.E., Forster, R.A. and Martz, R.L. (2012) MCNP Variance Reduction Developments in the 21st Century. Los Alamos National Lab (LANL), Los Alamos. <https://doi.org/10.2172/1054246>
- [58] Booth, T.E. (1985) A Sample Problem for Variance Reduction in MCNP. LA-10363-MS.